Materials Chemistry Horizons **RESEARCH**

Simulation of the Effect of Gallium Arsenide/Aluminum Gallium Arsenide Multilayer Material Structure on LED Performance

Mohammad Kamali Moghaddam

Electrical Engineering Department, Hakim Sabzevari University, Sabzevar, Iran

***Corresponding author**: m.kamali1982@gmail.com (M. Kamali Moghaddam)

Mater. Chem. Horizons, 2023, 2(4), 293 -301 10.22128/MCH.2024.766.1052 OPEN ACCESS

ABSTRACT

In various research, the effect of different types of semiconductor materials on the performance of light diodes has been investigated. Gallium arsenide and aluminum gallium arsenide are among the materials used for light diodes. The use of multilayer structures in light-emitting diodes can help improve their performance; Because these structures can improve light radiation and convert more optimal energy into light. Researchers are optimizing and designing light-emitting diodes to increase light intensity with less energy consumption as light-emitting diodes gradually replace incandescent bulbs. In this study, multilayer photodiode structures using gallium arsenide/gallium aluminum arsenide semiconductors are investigated and simulated, and the results of the article show that multilayer photodiode structures with gallium arsenide/gallium aluminum arsenide semiconductors, by simulating and examining electric fields, potential, radiation intensity And the consumption power of light diodes helps to optimize and achieve optimal performance. This research can be a guide for the development and improvement of light diodes with less energy consumption and better performance.

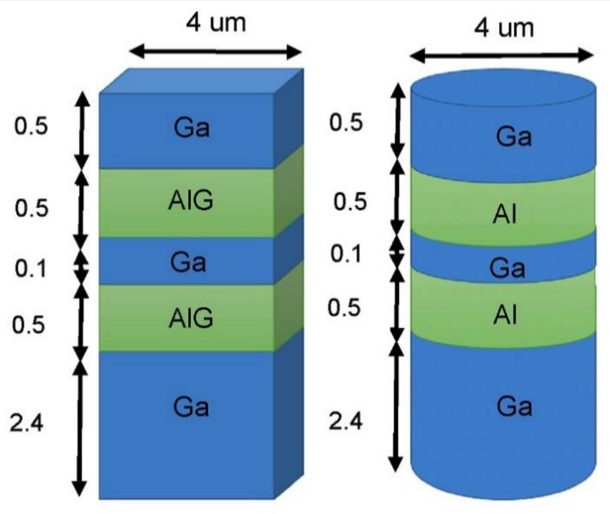

Keywords: Light diodes, gallium arsenide, aluminum gallium arsenide, radiation intensity

1. Introduction

The progress of light-emitting diodes is impressive [1-3]. During the survey conducted by Heitz in the last thirty years, the intensity of radiant light has doubled every twenty years, while the cost has decreased tenfold [4]. Now it has even exceeded these trends [5]. However, light-emitting diodes have been of particular interest for general lighting [3,6-12]. The efficiency of light-emitting diodes has reduced the operating voltage while maintaining the same current density and, as a result, the same brightness, which is mainly achieved by reducing the charge injection barriers and minimizing the thickness of the light-emitting diodes [13].

The intensity of a light source of any kind is evaluated using photometric techniques [14]. Visible light measurements are perceived by humans in the wavelength range of 830-360 nm. Light flux is introduced as the total light energy emitted per unit of time, and its unit is W/m^2. The intensities in the distinguishable range for humans are usually defined in terms of lumen unit, which is equivalent to the radiant flux of 1.683 W at the most sensitive wavelength for human vision, i.e. the wavelength of 555 nm (this value corresponds to photopic (day) vision, the maximum sensitivity for Scotopic vision (dark adaptation) occurs at 505 nm [14].

The growth of semiconductor layers in a light-emitting diode from semiconductor selective region materials composed of groups III-V of the periodic table has been studied for decades due to its numerous advantages in controlling the growth structure and morphology [15-20]. Meanwhile, the use of phosphide and arsenide materials from groups III-V respectively has been of interest, but on the other hand, there are fewer studies on the luminescent

Received: December 24, 2023
Received in revised: January 01, 2024
Accepted: January 05, 2024
This is an open access article under the CC BY license

properties of semiconductors such as aluminum gallium arsenide and gallium arsenide and their application in light diodes [20- 29] has been done. Until now, there has been interest in making small-dimension diodes of these materials, especially on the sub-millimeter scale, but recently there has been an increase in interest in the large-scale production of light-emitting diodes [30-32] (LED) and the development of high-power devices from these. We have been materials [33-39]. A deep understanding of geometrical effects on the properties of semiconductors such as aluminum gallium arsenide and gallium arsenide is necessary for application in optical devices, especially when parameters such as device scaling and array density become important [40]. Aluminum gallium arsenide semiconductors have direct energy gap and nonlinear electro-optical properties and perform in a wide range of applications, including quantum state generation, low-loss routing, electro-optical modulation, and on-chip single-photon detection [41-44].

Advances in the growth and fabrication of a variety of emerging photonic materials in the past decade have opened up many new and exciting opportunities for nonlinear integrated quantum photonics [45]. Aluminum gallium arsenide ternary alloys are prominent among the growing family of nonlinear photonic materials and are of great importance alongside dielectrics such as lithium niobate or lithium niobate on insulator (LNOI) and other III-V materials.

Using a high-quality molecular beam method with smooth atomic interfaces, GaAs/AlGaAs heterostructures can be grown with tunable composition and thickness to fabricate complex structures such as semiconductor diodes and lasers, such that the lattice constants of gallium arsenide. The lattice is maintained for all aluminum gallium arsenide compounds, thus enabling the defect-free growth of complex and heterogeneous multilayer structures [46-47].

Before the light diode or semiconductor piece enters the pre-fabrication and final commercial production stages, it is important to understand and review the theory and simulation of its features and performance, and this is very important in reducing costs and speeding up the process. Among the semiconductor device simulation software, TICD design software provides an effective tool for simulating semiconductor structures in steady state and transient conditions [48-50]. The analysis of electrothermal parameters such as electric field, leakage current, local heating, and network temperature is one of the capabilities of this software that can help to isolate structural vulnerability and understand the possible causes of device failure, and hence one of the most important and practical software. available for simulating semiconductor structures and electronic components is Silvaco-Atlas software, which also can be designed in nanometer dimensions [51].

2. Materials and methods

In this study, two rectangles and cylindrical structures are investigated. The dimensions of a rectangle structure with sides 4 micrometers long and a cylindrical structure with a diameter of 4 micrometers and a height of 4 micrometers are considered. As can be seen in **Figure 1**, both structures are made of 5 layers, the first layer is made of gallium arsenide with a thickness of 0.5 micrometers, and the second layer is made of aluminum gallium arsenide with a thickness of 0.5 micrometers. The third layer is less thick (0.1 micrometers) and is made of gallium arsenide, and the fourth layer is similar to the second layer, and the fifth layer is made of gallium arsenide with a thickness of 2.4 micrometers.

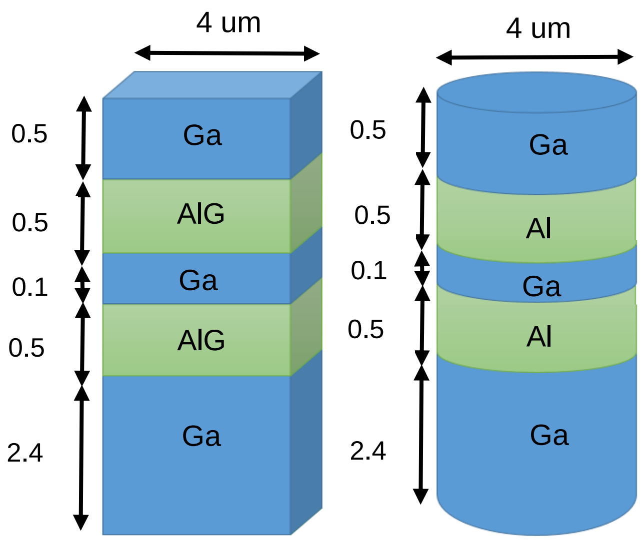

Figure 1. Cylindrical and rectangle light diode structure.

As seen in **Figure 2**, the simulated structure is shown in Silvaco software, in these structures, the anode electrode with a length of 1.5 micrometers is placed on top, and the cathode electrode is placed at the bottom of the structure with a length of 1.5 micrometers has taken.

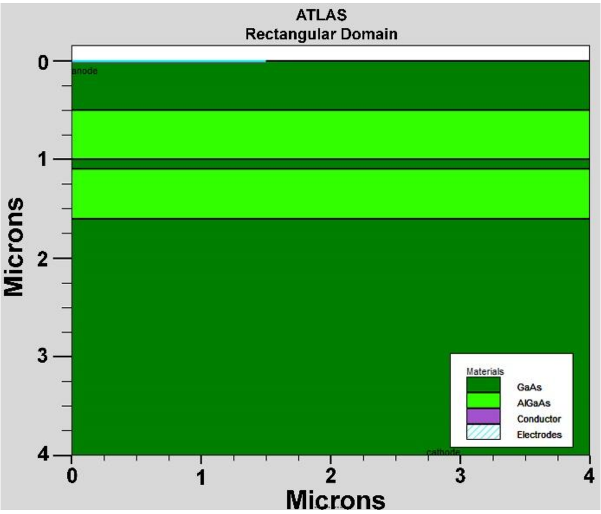

Figure 2. Simulated structure with Silvaco Atlas software

3. Results and discussion

In this study, two structures have been investigated. The first one is designed as a cylinder and the second one is designed as a cube, which is discussed in the structure section of the dimensional description of these structures. These structures have been simulated and analyzed by Silvaco Atlas software. For this software to have accurate calculations, we need to specify the required analytical models for it.

Light-emitting diodes are made of a special semiconductor compound that emits light in response to an electric current. In the design of light diodes, the Fermi model can be used to analyze the distribution of electrons and holes in the diode structure. This model can give us a better understanding of the electric current, the distribution of electrons and holes, and the production of light in light-emitting diodes. By using the Fermi model and other related models, it is possible to improve the performance characteristics of light-emitting diodes and make more optimal designs.

The Opto model is used in electronic and semiconductor simulation software, especially in Silvaco Atlas environments, to simulate optical structures and light diodes. This model can simulate optical effects in the presence of electron and hole flow in light diodes. Using the Opto model, it is possible to study the distribution of electrons and holes, light production, distribution of optical flux, optical efficiency, and other related characteristics in optical structures. This information can be used in the design and optimization of optical diodes and optical devices. In this simulation, for better analysis, models such as S-R-H and Agar are also used.

After simulating the models, the cathode and anode voltages are considered to be zero volts, then the anode voltage has been increased step by step with a value of 0.05 volts to reach the value of 2 volts. When the anode voltage increases step by step, the amount of light diode current and the amount of total illumination power are calculated concerning the increase in current. As **Figure 3** can be seen, it shows the changes in the anode current in terms of the changes in the anode-cathode voltage. From this diagram, it can be seen that the threshold voltage is almost equal in both forms, but when the light diode is turned on, the current of the cylindrical structure is more than the current of the rectangle structure.

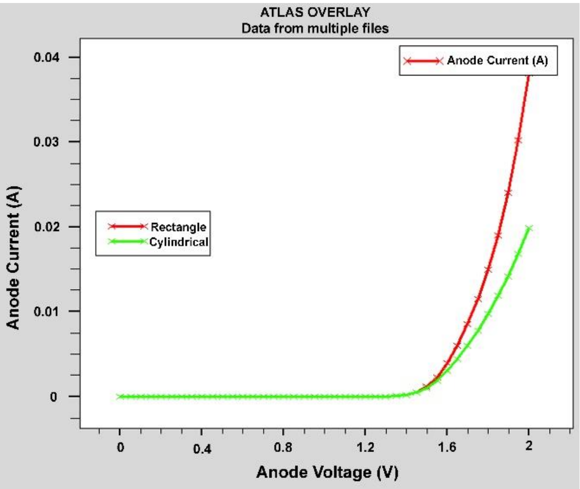

Figure 3. Graph of anode current versus anode-cathode voltage.

One of the significant values in light diodes and electrical elements is the on/off current ratio. To obtain the ratio of current on and off in this diagram, the ratio of the logarithm of current must be drawn in terms of voltage. In **Figure 4**, the logarithmic ratio of the current is drawn in terms of voltage, and as can be seen, the ratio of on-off current is slightly higher in the cylindrical structure than in the rectangle.

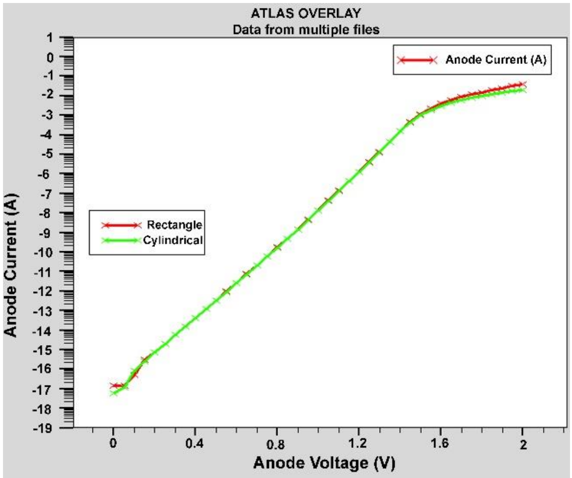

Figure 4. Graph of the logarithm of anode current versus anode-cathode voltage.

An important point that should be investigated in light-emitting diodes is the total lighting power of the light-emitting diode. As can be seen in **Figure 5**, the total lighting power of light diodes is shown in terms of changes. Therefore, according to the fact that the voltage of the two structures has been increased to 2 volts and it was shown in the previous diagram that the current of the cylindrical structure has increased to 40 milliamperes, but in the rectangle structure, the current has increased to 20 milliamperes.

Because it is not the user's hand to set the current, therefore, the diagram in **Figure 5** which is the exposure power of the light diode is drawn for a cylindrical structure up to a current of 40 milliamps (the same as 2 volts) and in a rectangle structure up to a current of 20 milliamps (the same as 2 volts). Is. Therefore, this diagram shows that the cylindrical structure is more than the rectangle structure in the voltage equal to the exposure power.

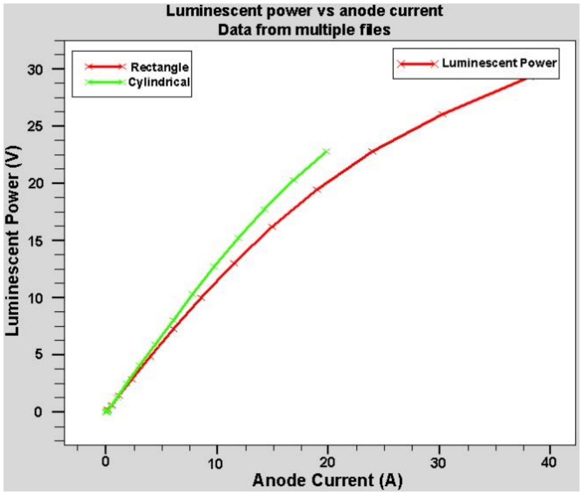

Figure 5. Radiant intensity diagram according to anode current.

For further investigation, a column cut was made in the middle (2 μm) of these structures. These cuts happened when the anode-cathode voltage was 2 volts. **Figures 6A** and **B** show the diagram of the electric field, which, as can be seen, in the places of semiconductor bonding, the cylindrical structure has a greater electric field than the rectangle one.

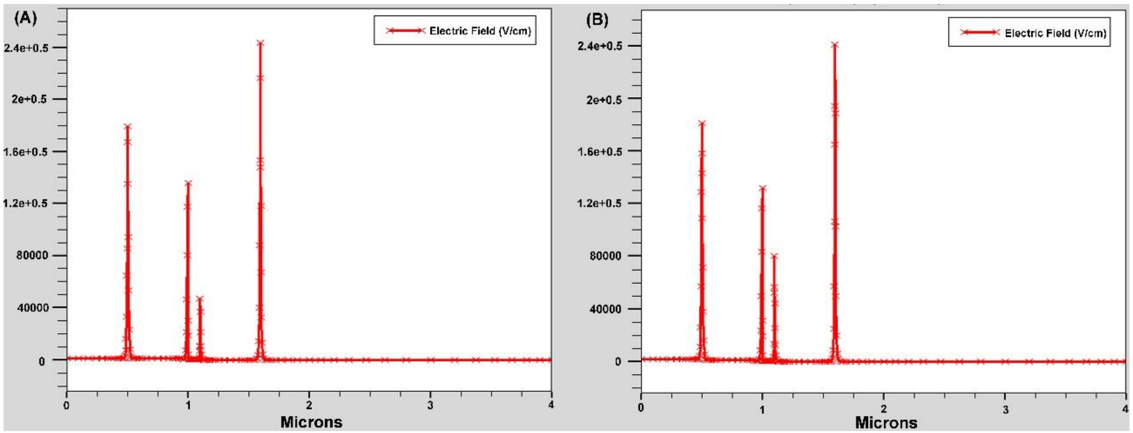

Figure 6. Diagram of the electric field along the (**A**) rectangle segment and (**B**) cylindrical piece.

Figures 7A and **B** in the same cut place show the potential diagram, which states that the potential is greater in the cylindrical state than in the rectangle one. From approximately 1.6 microns onwards, the potential is fixed and the field becomes zero.

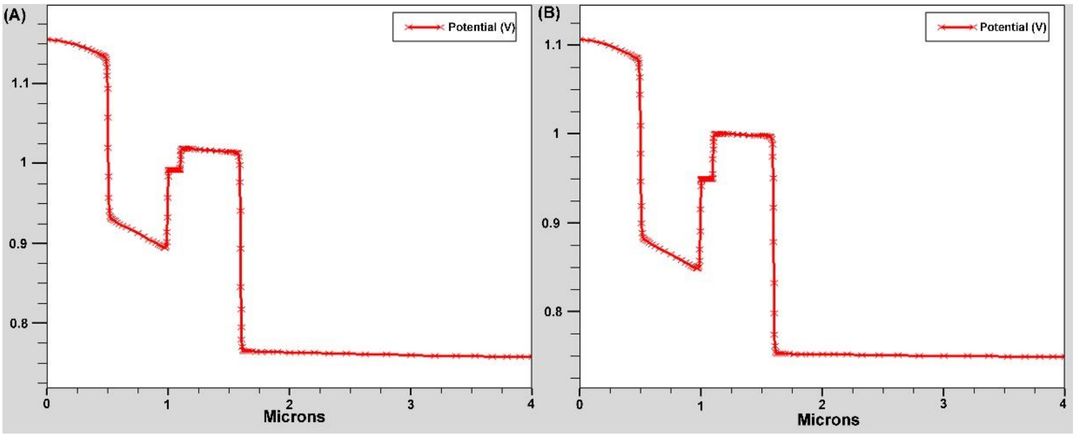

Figure 7. Potential diagram along the (**A**) rectangle segment and (**B**) cylindrical piece.

Figure 8A and **B** show the flow along the cut path. As can be seen from the graphs and results, in the cylindrical light diode at the same voltage, more current and as a result more light intensity is produced, and this indicates that with low power consumption, more light intensity can be achieved.

As can be seen in **Table 1**, under equal conditions, the amount of clear current is more in the cylindrical structure and as a result, the intensity of the current flow increases, this indicates that the cylindrical structure is better than the rectangle one.

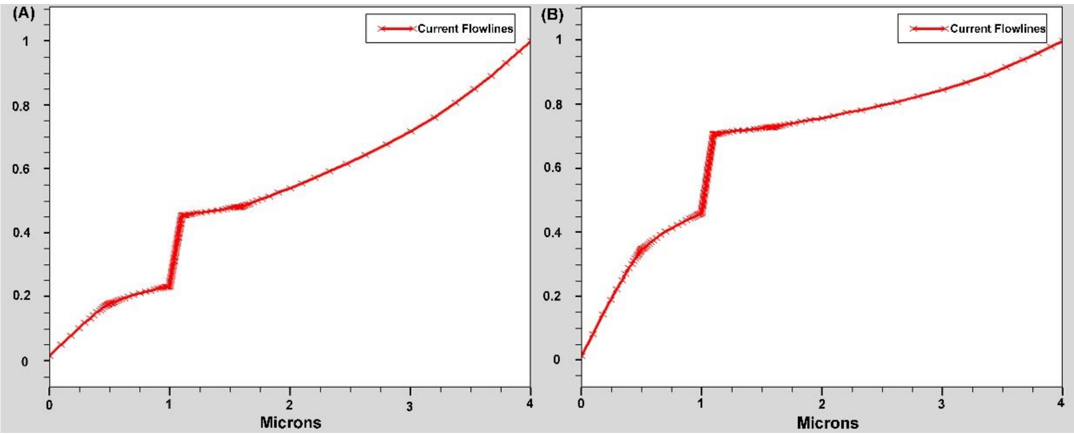

Figure 8. Current flow along the rectangle section (**A**) and (**B**) cylindrical part.

Table 1. Comparison of the results of two structures

Structures	Ion/Ioff	Vt	SS	Ion	Von
Cylindrical	15 order	1.6 V	50	20 mA	2 V
Rectangle	15.5 order	1.6 V	50	40 mA	2 V

4. Conclusions

Currently, the design and production of electronic components to reduce power consumption and increase efficiency have attracted a lot of attention. In this study, two photodiode structures have been investigated and compared to determine the best mode of use. To achieve this goal, the electric field, potential, intensity of electric current, current, and power consumption were studied and evaluated. The results showed that the cylindrical structure has more flow and electric current intensity than the rectangle structure. In addition, a higher on-off current ratio and lower power consumption were observed in the cylindrical structure compared to the rectangle structure, under the same conditions. These results can be used to improve the design and structure of light diodes as well as to reduce their energy consumption.

Authors' contributions

Not applicable.

Declaration of competing interest

Not applicable.

Funding

This paper received no funding.

Data availability

Data will be made available on request.

References

[1] B. Monemar, G. Pozina, Group III-nitride based hetero and quantum structures, Prog. Quantum Electron. 24 (2000) 239–290.
[2] E.F. Schubert, Light-Emitting Diodes, 2nd ed., Cambridge University Press, 2006.
[3] A. Zukauskas, M.S. Shur, R. Gaska, Introduction to Solid State Lighting, Wiley-Interscience, New York, 2002.
[4] F. Wall, P.S. Martin, G. Harber, High-power LED package requirements, Proc. SPIE 5187 (2004) 85–92.
[5] Z. Liu, S. Liu, K. Wang, X. Luo, Status and prospects for phosphor-based white LED packaging, Front. Optoelectron. China 2 (2009) 119–140.
[6] Slocum, A. (2005). A technology assessment of light emitting diode (LED) solid-state lighting for general illumination (No. 2168-2018-8077).
[7] S. Muthu, F.J.P. Schuurmans, M.D. Pashley, Red, green and blue LEDs for white light illumination, IEEE J. Selected Topics Quantum Electron. 8 (2002) 333–338.
[8] A. Mills, Lighting: the progress and promise of LEDs, III–V, Review 17 (2004) 39–41.
[9] N. Narendran, Y. Gu, J.P. Freyssnier, H. Yu, L. Deng, Solid-state lighting: failure analysis of white LEDs, J. Crystal Growth 268 (2004) 449–456.
[10] N. Narendran, Improved performance white LED, Proc. SPIE 5941 (2005) 594108.
[11] M.G. Craford, LEDs for solid state lighting and other emerging applications: status, trends and challenges, Proc. SPIE 5941 (2005) 594101.
[12] E.F. Schubert, J.K. Kim, Solid-state light sources getting smart, Science 308 (2005) 1274–1278.
[13] A.I. Zhmakin, Enhancement of light extraction from light emitting diodes. Physics Reports, 498 (2011) 189-241.
[14] Y. Ohno, Optical metrology for LEDs and solid state lighting, Proc. SPIE 6046 (2006) 604625.
[15] W. Bergbauer, Continuous-flux MOVPE growth of position-controlled N-face GaN nanorods and embedded InGaN quantum wells. Nanotechnology 21(2010) 305201.
[16] W.Bergbauer, N-face GaN nanorods: Continuous-flux MOVPE growth and morphological properties. J. Cryst. Growth 315 (2011) 164–167.
[17] K. Choi, M. Arita, Y. Arakawa, Selective-area growth of thin GaN nanowires by MOCVD. J. Cryst. Growth 357 (2012) 58–61.
[18] S. D.Hersee, X. Sun, X. Wang, The controlled growth of GaN nanowires. Nano Lett. 6 (2006)1808–11.
[19] K. Hiramatsu, Fabrication and characterization of low defect density GaN using facet-controlled epitaxial lateral overgrowth (FACELO). J. Cryst. Growth 221 (2000) 316–326.
[20] A.Lundskog, Controlled growth of hexagonal GaN pyramids by hot-wall MOCVD. J. Cryst. Growth 363 (2013) 287–293.
[21] S. Tanaka, Y. Kawaguchi, N. Sawaki, M. Hibino, K. Hiramatsu, Defect structure in selective area growth GaN pyramid on (111)Si substrate. Appl. Phys. Lett. 76 (2000) 2701.
[22] T.S. Zheleva, O. Nam, M.D. Bremser, R.F. Davis, Dislocation density reduction via lateral epitaxy in selectively grown GaN structures. Appl. Phys. Lett. 71(1997) 2472 .
[23] A.Chandolu, Selective Area Growth of GaN Nano Islands by Metal Organic Chemical Vapor Deposition: Experiments and Computer Simulations. MRS Proc. 955 (2011) I07–114.
[24] V. Kachkanov, Structural dynamics of GaN microcrystals in Evolutionary Selection Selective Area Growth probed by X-ray microdiffraction. Sci. Rep. 4(2014)4651.
[25] D. Kapolnek, Anisotropic epitaxial lateral growth in GaN selective area epitaxy. Appl. Phys. Lett. 71(1997) 1204.
[26] Y. Kawaguchi, Selective Area Growth of GaN on Si Substrate Using SiO2 Mask by Metalorganic Vapor Phase Epitaxy. Jpn. J. Appl. Phys. 37 (1998) L966–L969.
[27] X. Li, Characteristics of GaN stripes grown by selective-area metalorganic chemical vapor deposition. J. Electron. Mater. 26(1997) 306–310
[28] S. Okada, H. Miyake, K. Hiramatsu, Y. Enatsu, S. Nagao, Selective-area growth of GaN on non- and semi-polar bulk GaN substrates. Jpn. J. Appl. Phys. 53(2014) 05FL04
[29] Y. Wang, F. Hu, K. Hane, Lateral epitaxial overgrowth of GaN on a patterned GaN-on-silicon substrate by molecular beam epitaxy. Semicond. Sci. Technol. 27 (2011) 024008.
[30] Z.J. Liu, T. Huang, J. Ma, C. Liu, K.M. Lau, Monolithic Integration of AlGaN/GaN HEMT on LED by MOCVD. IEEE Electron Device Lett. 35 (2014) 330–332.
[31] B. Zhang, High-performance III-nitride blue LEDs grown and fabricated on patterned Si substrates. J. Cryst. Growth 298, (2007) 725–730.
[32] D. Zhu, D. Wallis, C. J. Humphreys, Prospects of III-nitride optoelectronics grown on Si. Rep. Prog. Phys. 76 (2013) 106501.
[33] M. Ishida, T. Ueda, T. Tanaka, D. Ueda, GaN on Si Technologies for Power Switching Devices. IEEE Trans. Electron Devices 60 (2013) 3053–3059.
[34] S. Musumeci, V. Barba, Gallium Nitride Power Devices in Power Electronics Applications: State of Art and Perspectives. Energies 16 (2023) 3894.
[35] Y. Zhang, Electrothermal Simulation and Thermal Performance Study of GaN Vertical and Lateral Power Transistors. IEEE Trans. Electron Devices 60 (2013) 2224–2230.
[36] S. Chowdhury, B.L. Swenson, M.H. Wong, & U.K.Mishra, Current status and scope of gallium nitride-based vertical transistors for high-power electronics application. Semicond. Sci. Technol. 28 (2013) 074014.
[37] J.L. Hudgins, G.S. Simin, E. Santi, M.A. Khan, An assessment of wide bandgap semiconductors for power devices. IEEE Trans. Power Electron. 18 (2003), 907–914.

[38] P. Srivastava, Record Breakdown Voltage (2200 V) of GaN DHFETs on Si With 2-μm Buffer Thickness by Local Substrate Removal. IEEE Electron Device Lett. 32 (2011) 30–32.
[39] M.J. Scott, Merits of gallium nitride based power conversion. Semicond. Sci. Technol. 28(2013) 074013.
[40] A.Tanaka, R. Chen, K. Jungjohann, Strong Geometrical Effects in Submillimeter Selective Area Growth and Light Extraction of GaN Light Emitting Diodes on Sapphire. Sci Rep 5(2015) 17314.
[41] C. P. Dietrich, A. Fiore, M. G. Thompson, M. Kamp, and S. Höfling, GaAs integrated quantum photonics: Towards compact and multi-functional quantum photonic integrated circuits, Laser Photon. Rev. 10 (2016) 870–894.
[42] A. Orieux, M. A. M. Versteegh, K. D. Jöns, and S. Ducci, Semiconductor devices for entangled photon pair generation: a review, Rep. Prog. Phys. 80 (2017) 076001.
[43] M. Schwartz, E. Schmidt, U. Rengstl, F. Hornung, S. Hepp, S. L. Portalupi, K. Llin, M. Jetter, M. Siegel, and P. Michler, Fully on-chip single-photon Hanbury-Brown and Twiss experiment on a monolithic semiconductor–superconductor platform, Nano Lett. 18 (2018) 6892–6897.
[44] C. McDonald, G. Moody, S. W. Nam, R. P. Mirin, J. M. Shainline, A. McCaughan, S. Buckley, and K. L. Silverman, III–V photonic integrated circuit with waveguide-coupled light-emitting diodes and WSi superconducting single-photon detectors, Appl. Phys. Lett. 115 (2019) 081105.
[45] S. Bogdanov, M. Y. Shalaginov, A. Boltasseva, and V. M. Shalaev, Material platforms for integrated quantum photonics, Opt. Mater. Express 7 (2017) 111–132.
[46] E. Mobini, D. H. G. Espinosa, K. Vyas, and K. Dolgaleva, AlGaAs nonlinear integrated photonics, Micromachines 13 (2020) 991 (2022).
[47] F. Baboux, G. Moody, S. Ducci, S. Nonlinear integrated quantum photonics with AlGaAs. Optica, 10 (2023) 917-931.
[48] M. Kamali Moghaddam, M. Moslemi, M. Farzaneh. Analytical Modeling of ZrO2, HfO2 and SiO2 Effect over Tunneling Field Effect Transistor. J. Electron. Mater. 49 (2020), 1467-1472.
[49] S.E. Hosseini, M.N. Moghaddam (2015). Analytical modeling of a pnin tunneling field effect transistor. Mater. Sci. Semicond. Process. 30 (2015) 56-61.
[50] M. Kamali, S.E. Hosseini. Investigation of a SiGe tunnel FET: comparison to Si and Ge TFETs. J. Electr. Syst. 2(2014), 21-26.
[51] S. Kaiser, F. Symalla, T. Neumann, A. Plews, D. Vander Velpen, F. Vandeplas, A.Nejim. Automated Multiscale Design Flow for Organic LED Design. In Electrochemical Society Meeting Abstracts. J. Electrochem. Soc. 239 (2021) 1059-1059.